CM² MAGAZINE

第 127 期

南方科技大学海洋磁学中心主编

http://cm2.sustech.edu.cn/

创刊词

海洋是生命的摇篮，是文明的纽带。地球上最早的生命诞生于海洋，海洋里的生命最终进化成了人类，人类的文化融合又通过海洋得以实现。人因海而兴。

人类对海洋的探索从未停止。从远古时代美丽的神话传说，到麦哲伦的全球航行，再到现代对大洋的科学钻探计划，海洋逐渐从人类敬畏崇拜幻想的精神寄托演变成可以开发利用与科学研究的客观存在。其中，上个世纪与太空探索同步发展的大洋科学钻探计划将人类对海洋的认知推向了崭新的纬度：深海（deep sea）与深时（deep time）。大洋钻探计划让人类知道，奔流不息的大海之下，埋藏的却是亿万年的地球历史。它们记录了地球板块的运动，从而使板块构造学说得到证实；它们记录了地球环境的演变，从而让古海洋学方兴未艾。

在探索海洋的悠久历史中，从大航海时代的导航，到大洋钻探计划中不可或缺的磁性地层学，磁学发挥了不可替代的作用。这不是偶然，因为从微观到宏观，磁性是最基本的物理属性之一，可以说，万物皆有磁性。基于课题组的学科背景和对海洋的理解，我们对海洋的探索以磁学为主要手段，海洋磁学中心因此而生。

海洋磁学中心，简称 CM^2，一为其全名“Centre for Marine Magnetism”的缩写，另者恰与爱因斯坦著名的质能方程 $E = MC^2$ 对称，借以表达我们对科学巨匠的敬仰和对科学的不懈追求。

然而科学从来不是单打独斗的产物。我们以磁学为研究海洋的主攻利器，但绝不仅限于磁学。凡与磁学相关的领域均是我们关注的重点。为了跟踪反映国内外地球科学特别是与磁学有关的地球科学领域的最新研究进展，海洋磁学中心特地主办 CM^2 Magazine，以期与各位地球科学工作者相互交流学习、合作共进！

“海洋孕育了生命，联通了世界，促进了发展”。21 世纪是海洋科学的时代，由陆向海，让我们携手迈进中国海洋科学的黄金时代。

目录

1. 绕极深层水的极向移动威胁东南极冰盖

翻译人：仲义 zhongy@sustech.edu.cn

Herraiz-Borreguero L, Garabato A C N, et al. ***Poleward shift of Circumpolar Deep Water threatens the East Antarctic Ice Sheet*** *[J] Nature Climate Change, 2022.*

https://doi.org/10.1038/s41558-022-01424-3

摘要：未来关于海平面上升预估具有很大的不确定性，主要是由南极冰盖对于气候变化的未知响应所导致。在过去四十年间，东南极冰盖对于海平面升高的贡献不断增加。然而，与南极西部不同的是，南极东部冰盖消失的原因在很大程度上尚未被探索。本文中，作者利用南极洲东部（80-160°E）附近的海洋观测资料证实，在 1930-1990 年和 2010-2018 年期间，沿大陆坡的中深度绕极深水温度上升了 0.8-2.0°C。研究结果表明，这种变暖可能与南极东部冰盖的损失和沿海水体的重组有关。此外，它还与南大洋地区夏季西风带每隔 10 年向极地移动有关。由于这种变化预计将持续到 21 世纪，因此，南极洲东部的海洋热量供应可能会继续增加，威胁到冰盖未来的稳定性。

ABSTRACT: Future sea-level rise projections carry large uncertainties, mainly driven by the unknown response of the Antarctic Ice Sheet to climate change. During the past four decades, the contribution of the East Antarctic Ice Sheet to sea-level rise has increased. However, unlike for West Antarctica, the causes of East Antarctic ice-mass loss are largely unexplored. Here, using oceanographic observations off East Antarctica (80–160° E) we show that mid-depth Circumpolar Deep Water has warmed by 0.8–2.0 °C along the continental slope between 1930–1990 and 2010–2018. Our results indicate that this warming may be implicated in East Antarctic ice-mass loss and coastal water-mass reorganization. Further, it is associated with an interdecadal, summer-focused poleward shift of the westerlies over the Southern Ocean. Since this shift is predicted to persist into the twenty-first century, the oceanic heat supply to East Antarctica may continue to intensify, threatening the ice sheet's future stability.

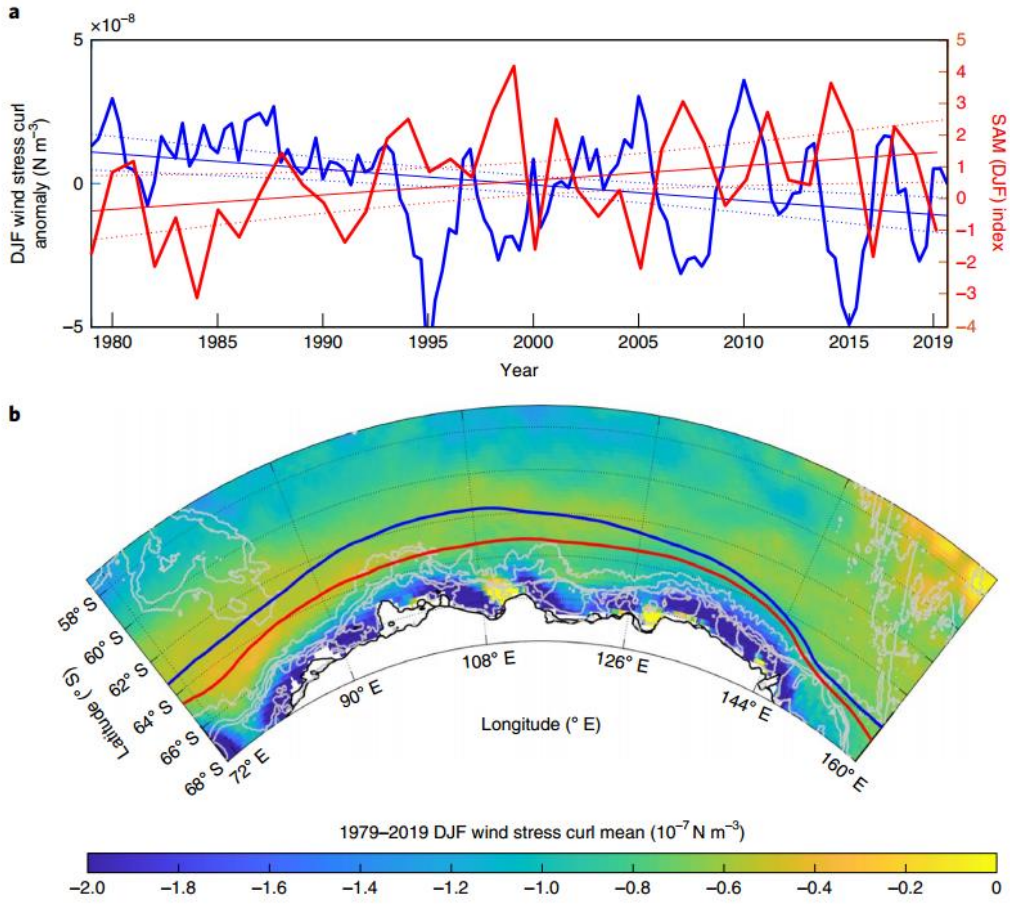

Figure 1. Changes in WSC and their link to the southward migration of the S-ACC. a, Summer (December–February) WSC anomaly relative to the time mean over the 1979–2018 period over 59–62° S/80–150° E (blue) (Supplementary Fig. 12). The blue thin line is the linear regression fit (which has a slope of -1.81×10^{-10} N m^{-3} per decade, $P < 0.01$), bounded by 95% confidence bounds (blue dashed lines). The red line is the Marshall SAM summer (December–February) index and the thin red line shows the positive trend (P= approximately 0.03, bounded by 95% confidence bounds) in that index. b, 1979–2018 mean summer (December–February) WSC (N m^{-3}) in the eastern Indian Ocean sector of the Southern Ocean. The black and red contours indicate the location at which the meridional WSC is zero in 1980–1985 and 2010–2015, respectively. The 400-, 1,000-, 2,000- and 3,000-m isobaths are shown as grey line

2. 伦敦空气中纳米物质的磁学性质

翻译人：张琪 zhangq7@sustech.edu.cn

Muxworthy A, Lam C, Grenn D, et al. ***Magnetic characterisation of London's airborne nanoparticulate matter*** *[J] Atmospheric Environment, 2022, 287, 119292.*

https://doi.org/ 10.1016/j.atmosenv.2022.119292

摘要：众所周知，汽车排放产生的含铁颗粒物是有毒的。为了更好地量化其潜在的健康风险，作者首次对伦敦可吸入颗粒物（<10 μm, PM_{10}）进行了磁性研究，该研究所用样品来自 2010 年和 2012 年伦敦市中心的三个监测站（Marylebone Road, Earl's Court Road 和 Oxford Street）。作者对所有样品进行了室温下的分析，少数样品在高温和低温下都进行了分析。高温测得磁铁矿为主要载磁矿物。低温测量显示，大量的纳米磁铁矿颗粒在 1-4 nm 的粒度范围内。据估计，在 10 K 时，多达 40%的总磁信号来自于小于 4 纳米的颗粒，这些颗粒在室温下是“不可见的”，因此在基于室温的磁学研究中经常被低估。低温测得的磁铁矿总浓度约为 7.5%，比先前报道的数值高得多。将室温磁学数据与 NO_X、PM_{10} 等污染数据及气象数据进行比较，发现饱和磁化强度等与质量相关的指标与 NO_X 和 PM_{10} 有很强的相关性，表明这些污染物有一个共同的来源，即车辆排放。磁性矫顽力测量与含量无关，可提供粒度信息，在所有三个取样地点数据具有一致性，再次表明他们存在一个主要来源。相对较小的矫顽力的变化与气象事件（如温度和降水）有关，表明空气中较大的颗粒（如>50 nm）优先的被去除掉了。

ABSTRACT: Iron-bearing particulate matter produced by vehicle emissions is known to be toxic. To better quantify potential health risks, we have conducted the first magnetic study of a time-series of London's inhalable particulate matter (<10 μm, PM_{10}), captured by three monitoring stations in central London (Marylebone Road, Earl's Court Road and Oxford Street) through 2010 and 2012. We conducted room-temperature analysis on all the samples, and a limited number of samples were analysed at both high and low temperatures. The high-temperature measurements identified magnetite as the dominant magnetic phase. The low-temperature measurements revealed high numbers of nanoparticles, which, assuming magnetite, are in the grain-size range 1–4 nm. It is

estimated that as much as ~40% of the total magnetic signal at 10 K is from particles <4 nm, that are magnetically 'invisible' at room-temperature and are being routinely under-estimated in room temperature-based magnetic studies. From the low-temperature measurements, the total concentration of magnetite was estimated at ~7.5%, significantly higher than previously reported. The room-temperature magnetic data were compared with other pollution data, e.g., NO_X and PM_{10}, and meteorological data. Mass-dependent terms like the saturation magnetisation were found to display a strong correlation with NO_X and PM_{10}, indicating a common source for these pollutants, i.e., vehicle emissions. Magnetic coercivity measurements, which are independent of abundance, and provide information on grain-size, were consistent across all three sampling localities, again suggesting a major dominant source. Relatively small variations in coercivity were correlated with meteorological events, e.g., temperature and precipitation, suggesting preferential removal of larger airborne grains, i.e., >50 nm.

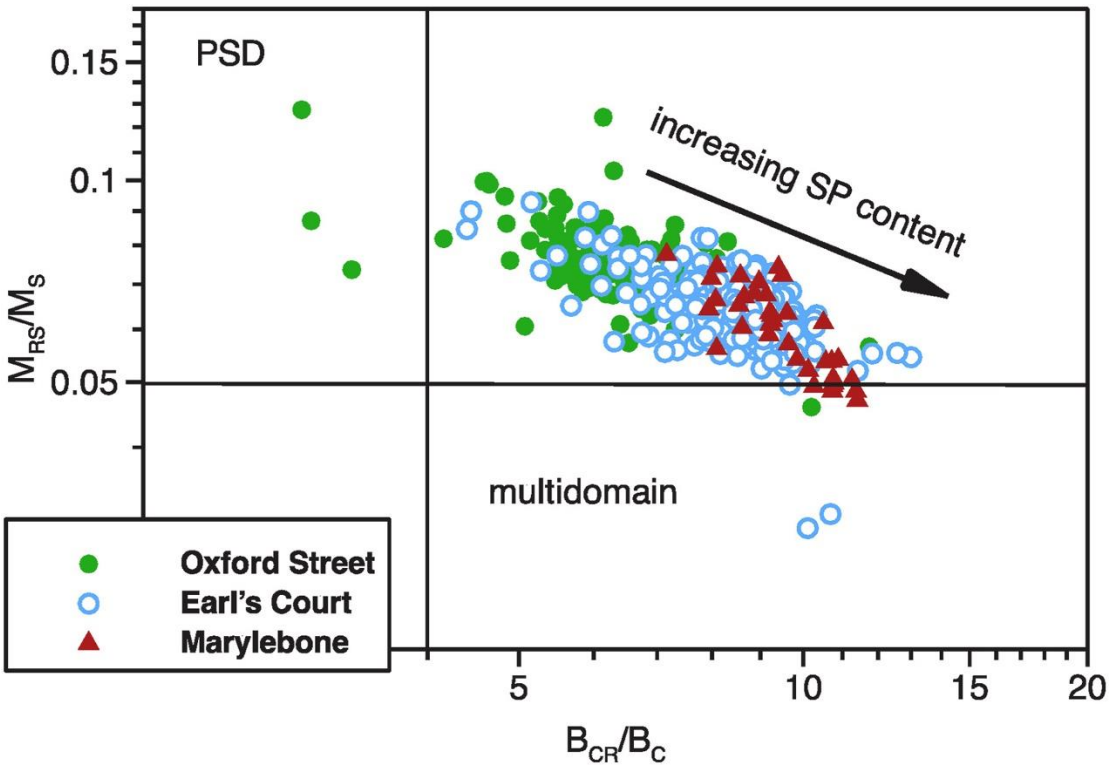

Figure 1. A 'Day' plot (Day et al., 1977) of MRS/MS versus HCR/HC for data from the Oxford Street, Marylebone Road and Earl's Court Road sites. To enhance the visual variation between the samples, only a sub-area of the 'typical' Day plot is shown. The PSD (100–1000 nm for magnetite) and MD (>1000 nm for magnetite) domain state regions are marked, as is the superparamagnetic, SP (<30 nm for magnetite) trend.

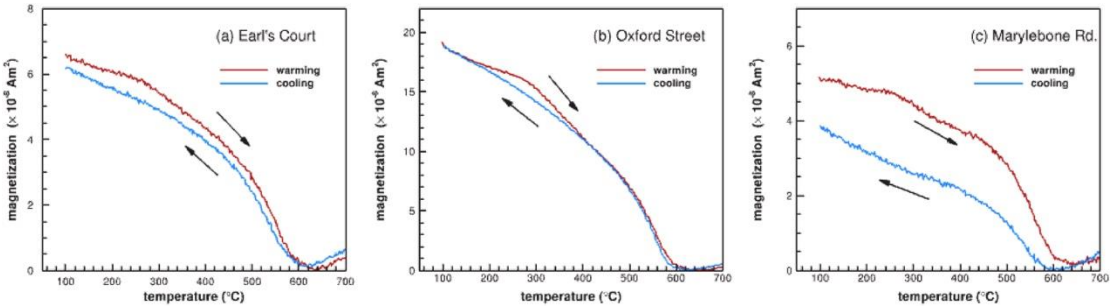

Figure 2. Thermomagnetic curves for the three localities: a) Earl's Court, b) Oxford Street and c) Marylebone Road. The PM_{10} was extracted from the filters by placing the filters in isopropanol in an ultrasonic bath for 30 min. About ~30 samples combined to produce enough material for these measurements. The applied field was 100 mT.

3. 中国东部边缘海海水中汞（Hg）的质量收支：沉积物-水传输过程的重要性

翻译人：张靖宇 zhangjy6@sustech.edu.cn

Chen L, Liu C, Yin Y, et al. ***Mass Budget of Mercury (Hg) in the Seawater of Eastern China Marginal Seas: Importance of the Sediment–Water Transport Processes*** *[J] Environmental Science & Technology, 2022.*

https://doi.org/10.1021/acs.est.2c03261

摘要：中国东部边缘海域（ECMS）一直面临各种环境问题，包括汞（Hg）污染。尽管以前的一些研究集中在 ECMS 的汞质量平衡方面，但汞在沉积物-水界面的迁移的贡献仍然不清楚。本研究旨在获取和量化沉积物-水传输过程在汞循环中的重要性。观察到上覆水和底层水的汞浓度与汞从沉积物到水中的扩散率之间存在明显的正相关关系。在冬季巡航中观察到整个水体中的 THg 浓度高出 2-3 倍，这应该是为了加强再悬浮过程。ECMS 中汞的质量收支进一步显示，扩散和再悬浮过程分别占 BS、YS 和 ECS 中总输入汞的 46%、60%和 16%。这些结果表明，沉积物-水传输过程在 ECMS 的汞循环中起着重要作用。作为 ECMS 中的一个重要的汞 "池"，汞在沉积物-水界面的迁移可能会影响这些系统中汞的长期风险评估。

ABSTRACT: The Eastern China Marginal Seas (ECMS) have been facing a variety of environmental problems, including mercury (Hg) pollution. Although several previous studies have been focused on mass balance of Hg in the ECMS, the contribution of Hg transport at the sediment–water interface remains unclear. This study was aimed to access and quantify the importance of sediment–water transport processes in Hg cycling. Significantly positive correlations were observed between Hg concentrations in the overlying and bottom water and the diffusion rates of Hg from sediment to the water. Approximately 2–3 times higher of THg concentrations in the entire water column were observed in a winter cruise with strong waves which was supposed to strengthen the resuspension process. The mass budget of Hg in the ECMS further showed that diffusion and resuspension processes accounted for approximate 46%, 60%, and 16% of total input Hg in the BS, YS, and ECS, respectively. These results suggest that the sediment–water transport processes play an important role in Hg cycling in the ECMS. As an important “pool” of Hg in the ECMS, the

transport of Hg at the sediment–water interface may affect the long-term risk assessment of Hg in these systems.

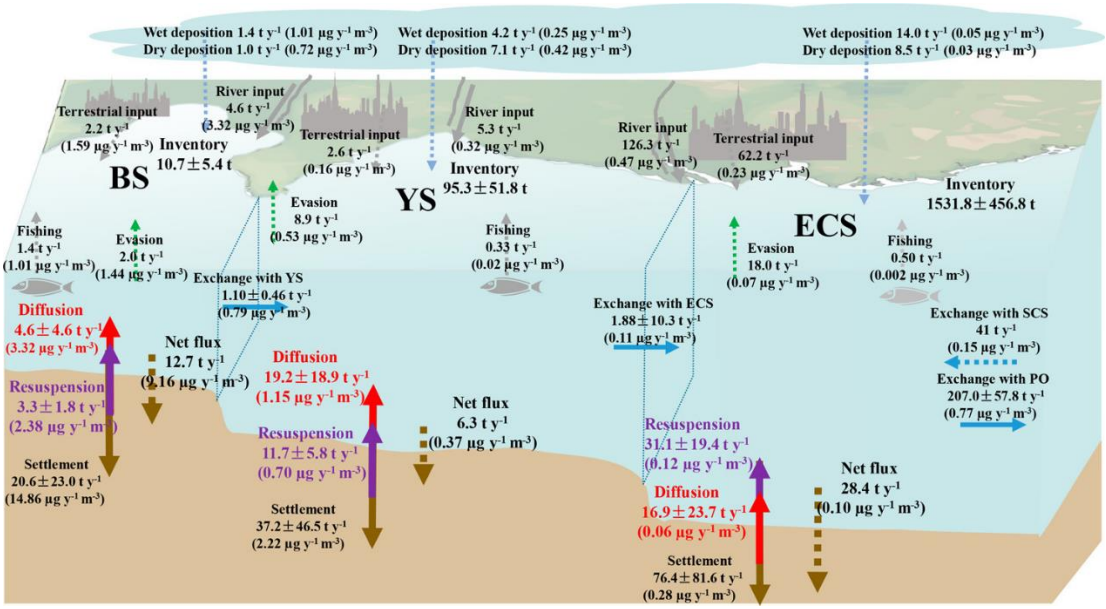

Figure 1. Mass budgets of Hg in the BS, YS, and ECS. Data cited from other sources (atmospheric deposition, evasion, fishing, and exchange with the South China Sea) were presented in dotted arrows.

4. 青藏高原南部414,000年来轨道尺度的水文气候变化

翻译人：杨会会 11849590@mail.sustech.edu.cn

Wang H B, Wang X Y, Perez-Mejias C, et al. ***Orbital-scale hydroclimate variations in the southern Tibetan Plateau over the past 414,000 years*** *[J] Quaternary Science Reviews. 2022, 291, 107658. https://doi.org/10.1016/j.quascirev.2022.107658*

摘要：石灰岩洞穴沉积物氧同位素($\delta^{18}O$)是广泛时间尺度上重建印度和东亚夏季风(ISM 和EASM)水文气候历史的重要指标之一。本文利用青藏高原中南部天门洞的3个新古洞穴$\delta^{18}O$记录，结合前人的记录，重建了一个距今414,000的合成天门洞洞穴记录。天门$\delta^{18}O$记录响应北半球夏季日照(NHSI)的变化，与ISM和EASM地区的洞穴$\delta^{18}O$记录基本一致。与以往的模拟和现代水文气候分析相比，天门$\delta^{18}O$记录主要被解释为指示ISM强度的指标。天门$\delta^{18}O$记录包含NHSI高、低两个时段，在岁差周期上变化幅度特别大(~14‰)，可能是降水量、水分来源、输运途径、高海拔和“雨出”效应等因素共同作用的结果。此外，天门$\delta^{18}O$、$\delta^{13}C$和微量元素记录的轨道尺度变化具有广泛的一致性，表明ISM的强度也调节了天门洞地区的有效降雨。值得注意的是，天门石笋的生长仅发生在温暖湿润的间冰期，甚至在接近岁差最大值的低NHSI时期，相反，在冷干的冰期持续出现中断。这种模式与在该地区发现的钙华岩层相似，都表明间冰期温度可能是该地区洞穴/钙华岩层形成的先决条件，而强的ISM降水反过来提供了充分条件。我们在天门的新记录，结合来自亚洲西风带和亚洲季风区的大量石笋记录，提供了进一步的证据来支持先前的假设:在广大范围的亚洲季风和西风带地区，轨道和千年尺度降水的$\delta^{18}O$具有一致的时间模式。因此，为了协调石笋和青藏高原冰芯揭示的降水$\delta^{18}O$变化，我们认为古里雅冰芯年代学的基础年龄可能为~70 ka BP，这与古里雅冰冠的最新测年结果一致。

ABSTRACT: Speleothem oxygen isotope ($\delta^{18}O$) constitutes one of key proxies to reconstruct the Indian and East Asian summer monsoon (ISM and EASM) hydroclimate history on a wide range of timescales. Here, we use three new well-dated speleothem $\delta^{18}O$ records from Tianmen cave, in the south-central Tibetan Plateau (TP), together with previous records from the same cave, to reconstruct a composite Tianmen record spanning over the past 414,000 years. The Tianmen $\delta^{18}O$

record follows Northern Hemisphere summer insolation (NHSI), broadly coherent with speleothem $\delta^{18}O$ records from both ISM and EASM regimes. In comparison with previous model simulations and modern hydroclimate analyses, the Tianmen $\delta^{18}O$ was interpreted primarily as a proxy indicating the ISM intensity. The Tianmen $\delta^{18}O$ record comprises both high and low NHSI time periods, which reveals an exceptional large amplitude (~14‰) of $\delta^{18}O$ variations at the precession band, possibly resulted from a combination effect of precipitation amount, moisture source, transport pathway, high elevation and rainout. Besides, a broad consistency on orbital-scale variability among Tianmen $\delta^{18}O$, $\delta^{13}C$ and trace element records is found, suggesting that the ISM intensity regulates the effective rainfall at the cave site as well. Notably, Tianmen speleothem growth occurred merely during warm-wet interglacial periods, even during low NHSI times near the precession maximum, and in contrast, hiatuses persistently occurred throughout cold-dry glacial periods. This pattern is similar to that found in travertine formations in the region, both suggesting that the interglacial temperature might be a prerequisite for speleothem/travertine formations in the region, while the strong ISM precipitation in turn provides a sufficient condition. Our new Tianmen record, combined with a large set of speleothem records from both Asian Westerlies and Asian monsoon domains, gives further evidence to reinforce a previous hypothesis: a consistent temporal pattern in the $\delta^{18}O$ of precipitation on orbital and millennial scales over the vast Asian monsoon and Westerlies regimes. As such, in order to reconcile the precipitation $\delta^{18}O$ variations between speleothem and TP ice cores, we argue that the Guliya ice-core chronology may have a basal age of ~70 ka BP, which is supported by recent dating results from the Guliya ice cap.

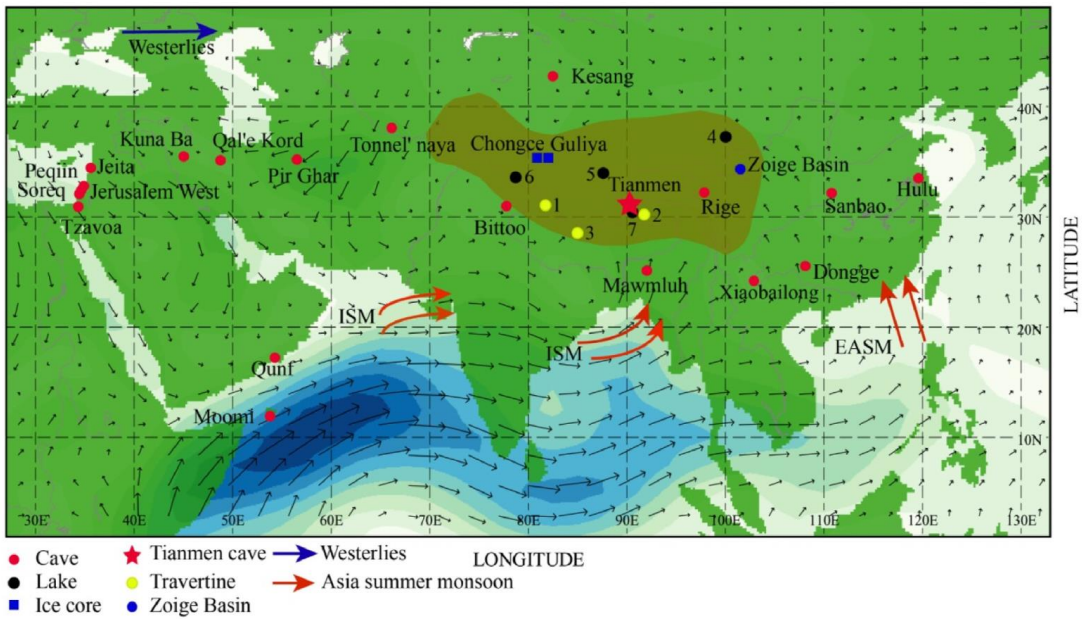

Figure 1. Location of study site and averaged wind field isobars at 850 hPa in summer (June to september) from 1980 to 2020. Arrows depict wind predominant direction of the Indian summer monsoon and East Asia summer monsoon (red) and the Westerlies (blue). Grey shadow area denotes the topography at 2500 m above sea level, indicating the delineation of the TP. The symbols represent the following archives: ice cores (blue squares), caves (red circles), travertines (yellow circles) and lakes (black circles). The red star points to Tianmen cave. The records cited are: Guliya ica core, Chongce ice core, Tianmen cave, Rige cave, Hulu cave, Sanbao cave, Kesang cave, Xiaobailong cave, Bittoo cave, Dongge cave, Tzavoa cave, Soreq cave, Peqiin cave, Jeita cave, Jerusalem cave, Kuna Ba cave, Qal'e Kord cave, Pir Ghar cave, Tonnel'naya cave, Moomi cave, Qunf cave, Mawmluh cave. Tirthapuri travertine (#1), Chusang travertine (#2), Nyalam travertine (#3). Lake Qinghai (#4), Linggo Co (#5), Bangong Co (#6), Nam Co (#7) and Zoige Basin (blue circle). (For interpretation of the references to color in this figure legend, the reader is referred to the Web version of this article.)

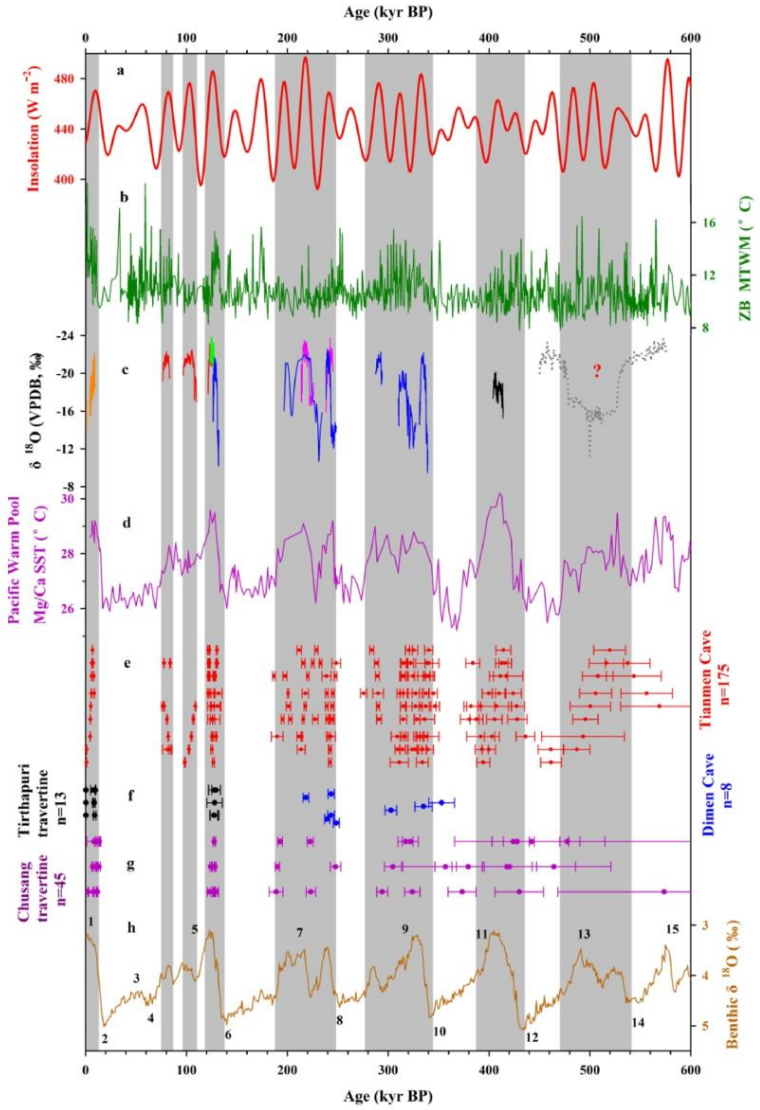

Figure 2. Comparison of multiproxy records: (a) 21 July insolation at 65 ℕ (Berger, 1978). (b) Reconstructed mean temperature of the warmest month, based on pollen data from Zoige Basin core ZB13-C2 (Zhao et al., 2020). (c) Tianmen $\delta^{18}O$ composite record (this study), the dotted grey line $\delta^{18}O$ record were from 19TM-2, this portion of the $d^{18}O$ record is not included in the composite profile, due to the large dating errors. (d) Pacific Mg/Ca-infered sea surface temperature (SST) (Medina-Elizalde and Lea, 2005). (e, f, g) ^{230}Th ages and 2s errors from Tianmen cave stalagmites (red), Tirthapuri travertine (black) (Wang et al., 2017), Dimen cave (~300 m west of Tianmen cave) stalagmites (blue) and Chusang travertine (purple) (Wang et al., 2022). (h) LR04 Benthic $d^{18}O$ stack (Lisiecki and Raymo, 2005), including MIS labels. Grey shadings show the growths periods of Tianmen speleothem. (For interpretation of the references to color in this figure legend, the reader is referred to the Web version of this article.)

5. 利用有孔虫保存指数量化底栖有孔虫的成岩作用、成因和由此产生的同位素偏差：对地球化学指标记录的影响

翻译人：王浩森 11930841@mail.sustech.edu.cn

Poirier R K, Gaetano M Q, Acevedo K, et al. ***Quantifying diagenesis, contributing factors, and resulting isotopic bias in benthic foraminifera using the Foraminiferal Preservation Index: Implications for geochemical proxy records*** *[J] Paleoceanography and Paleoclimatology, 2021, 36(5), e2020PA004110.*

https://doi.org/10.1029/2020PA004110

摘要：底栖有孔虫方解石测试的地球化学记录，特别是 *Cibicidoides* 属和 *Uvigerina* 属的地球化学记录，为重建过去的气候提供了基础。然而，底栖有孔虫受沉积后蚀变影响的程度没有受到很好的限制。此外，成岩作用如何改变底栖有孔虫测试的地球化学组成，从而使各种基于指标的气候记录产生偏差，也没有受到很好的限制。我们提出了有孔虫保存指数（FPI），作为一种新的指标，根据客观、明确的标准量化保存质量。FPI 用于识别和量化从上新世晚期到现代岩芯顶部样品（3.3–0 Ma）以及深海空间的成岩作用趋势。FPI 确定深海水团的化学成分是随着时间推移成岩作用作为主要驱动因素，同时也是确定水团影响变化周期的补充方法。此外，我们还提供了从具有不同保存质量的单个 Cibicidoides 样本中生成的稳定同位素数据（$\delta^{18}O$、$\delta^{13}C$），证明了各种地球化学指标记录中存在显著偏差的可能性，尤其是用于重建过去冰量和海平面变化的记录。这些单一测试数据进一步证明，结合最高保存质量的测试时，可以生成可靠的古记录。

ABSTRACT: Geochemical records generated from the calcite tests of benthic foraminifera, especially those of the genera *Cibicidoides* and *Uvigerina*, provide the basis for proxy reconstructions of past climate. However, the extent to which benthic foraminifera are affected by postdepositional alteration is poorly constrained. Furthermore, how diagenesis may alter the geochemical composition of benthic foraminiferal tests, and thereby biasing a variety of proxy-based climate records, is also poorly constrained. We present the Foraminiferal Preservation Index

(FPI) as a new metric to quantify preservation quality based on objective, well-defined criteria. The FPI is used to identify and quantify trends in diagenesis temporally, from late Pliocene to modern coretop samples (3.3–0 Ma), as well as spatially in the deep ocean. The FPI identifies the chemical composition of deep-ocean water masses to be the primary driver of diagenesis through time, while also serving as a supplementary method of identifying periods of changing water mass influence at a given site. Additionally, we present stable isotope data ($\delta^{18}O$, $\delta^{13}C$) generated from individual *Cibicidoides* specimens of various preservation quality that demonstrate the likelihood of significant biasing in a variety of geochemical proxy records, especially those used to reconstruct past changes in ice volume and sea level. These single-test data further demonstrate that when incorporating carefully selected tests of only the highest preservation quality, robust paleorecords can be generated.

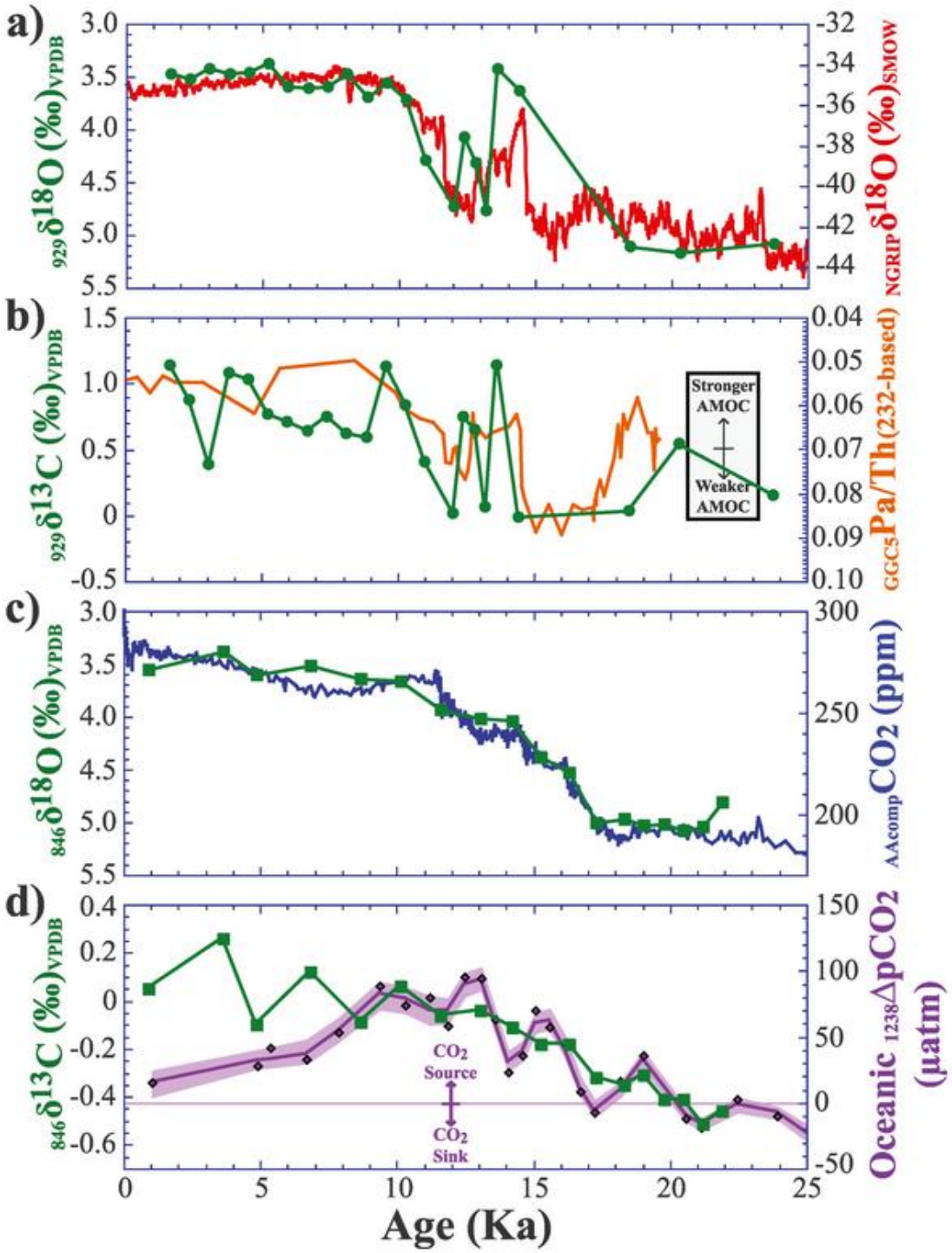

Figure 1. Comparisons of robust stable isotope data generated exclusively from well-preserved glassy *Cibicidoides* specimens from Site 929 compared to (a) the NGRIP ice core record (Andersen et al., 2006; Rasmussen et al., 2006; Svensson et al., 2006, 2008; Vinther et al., 2006) and (b) the Pa/Th record from the GGC5 site on the Bermuda Rise of McManus et al. (2004) and from Site 846 compared to (c) the Antarctic composite ice core CO_2 record (Bereiter et al., 2015) and (d) the surface ocean ΔpCO_2 record from Site 1238 (Martínez-Botí et al., 2015).

6. 通过潘培黄土的物源揭示南半球晚第四纪大气环流

翻译人：王敦繁 Dunfan-w@foxmail.com

Torre G, Gaiero D, Coppo R, et al. ***Unraveling late Quaternary atmospheric circulation in the Southern Hemisphere through the provenance of Pampean loess*** *[J] Earth-science Reviews, 2022, 232.*

https://doi.org/ 10.1016/j.earscirev.2022.104143

摘要：潘培黄土是南半球最广泛的大陆风成物质的古记录，记录了由南纬西风和亚热带急流两大纬向风系统搬运的沙尘沉积。本文对阿根廷中部潘潘地区黄土带 700 km 范围内的 3 个晚更新世-早全新世剖面的 REE、Nd、Sr 和 Pb 同位素进行了分析，以提高对南半球古大气环流的认识。3 个剖面与南美南部(SSA)潜在沙尘源的同位素对比表明: (1)高原南部至巴塔哥尼亚北部纬度地区的沙尘源为潘帕斯草原提供了沙尘;(2)细粒黄土和粗粒黄土 Sr-Nd 同位素的微小差异可能是由于粒度效应，而非物源差异;(3)在 43 ~ 41 ka BP、20 ~ 18 ka BP、14.6 ~ 12.6 ka BP 和 11.4 ~ 8.9 ka BP 期间，高原南部和普纳南部的沙尘堆积率增加。我们将这些大陆沙尘通量的上升与 Puna-Altiplano 高原从湿润到干燥的气候转变联系在一起，这与潘潘平原同步向湿润条件的气候转变有关，可能是由厄尔尼诺触发的。与现代 SSA 沙尘的同位素对比表明，其物源与古沙尘记录相似，表明 MIS 3 至现代的沙尘源基本不变，不同沙尘源的活化/失活导致地球化学特征变化不大。此外，将黄土剖面的同位素特征与更远端的古档案(即南大西洋海洋沉积物岩芯和南极冰芯)进行对比，表明与以前的观点相反，潘潘黄土不是这些地区的重要沙尘来源。此外，寒冷时期常见的尘埃来源(例如，末次冰期最大值和南极寒冷逆转)支持了这样一种观点，即大气传输效率的变化比物源的变化更能解释遥远古档案中在冰期/间冰期观测到的尘埃通量变化。

ABSTRACT: The Pampean loess is the most extensive continental paleo-record of aeolian material in the Southern Hemisphere, recording the deposition of dust transported by two major zonal wind systems: the southern westerly winds and the subtropical jets. In order to increase the understanding on paleo-atmospheric circulation over the Southern Hemisphere, we evaluate dust provenance through REE, Nd, Sr and Pb isotopes in three sections deposited during late Pleistocene-early

Holocene across 700 km in the loess belt of the Pampean region in central Argentina. The isotopic comparison of loess from the three sections with southern South American (SSA) potential dust sources show that (1) sources from the southern Altiplano to latitudes of northern Patagonia supplied dust to the Pampas, (2) the slight Sr– Nd isotopic difference between fine and coarse loess may be attributable to grain size effects rather than to differences in provenance, and (3) higher mass accumulation rates in the Pampas are associated with an increased presence of dust originated in the southern Altiplano and southern Puna during the spans of 43–41 ka BP, 20–18 ka BP, 14.6–12.6 ka BP and 11.4–8.9 ka BP. We associate these rises in con- tinental dust fluxes with climatic transitions from wetter to drier periods in the Puna-Altiplano Plateau related to synchronous climatic shifts to humid conditions at the Pampean Plain, probably triggered by El Nin˜o-like conditions. The isotopic comparison with modern SSA dust indicates similar provenance compared to paleo-dust records, suggesting almost constant dust sources from MIS 3 to modern times and/or modest changes in the geochemical signature under the activation/deactivation of the different dust sources. Moreover, contrasting the isotopic signature of the loess sections with more distal palaeoarchives (i.e., South Atlantic Ocean marine sediment cores and Antarctic ice cores), the new data suggest that contrary to previous ideas, the Pampean Loess was not an important source of dust to these regions. Also, a common dust provenance during cold periods (e.g., Last Glacial Maximum and Antarctic Cold Reversal) supports the idea that changes in atmospheric transport efficiency can better explain dust flux variations observed over glacial/interglacial periods in distant palaeoarchives than changes in provenance.

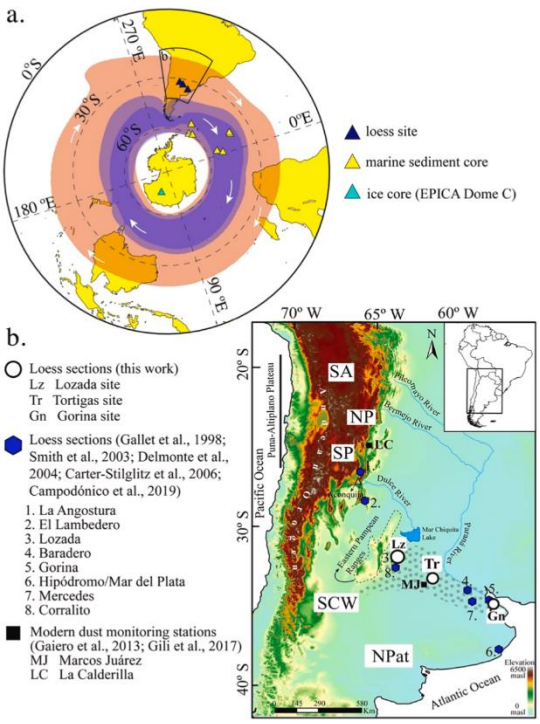

Figure 1. (a) Map showing the location of dust records and main wind belts from the Southern Hemisphere discussed in this paper. The lighter and darker blue-purple areas are delimited by the 7 ms^{-1} and 10 ms^{-1} contours of the E-W wind component at 850 hPa, respectively, and represent the South Westerly Winds. In turn, the reddish area is delimited by the 18 ms^{-1} contours of the E-W wind component at 200 hPa, and represents the Sub-Tropical Jet. In all cases, contours represent the 1979–2020 climatological means calculated from monthly ERA5 reanalysis data. White arrows indicate general wind direction. (b) Map showing the location of the three loess sections studied in this work (white dots): Lz, Lozada; Tr, Tortugas and Gn, Gorina. The dotted area indicates the limits of the "loessic/loessoide" or "loess belt" sector of the Pampean region. The black squares are the present-day dust monitoring stations. Blue symbols indicate previously studied loess sites with available geochemical data.

7. 墨西哥 Popocatépetl 火山碎屑沉积的居里温度和就位条件

翻译人：张伟杰 12031188@mail.sustech.edu.cn

Dudzisz K, Kontny A, Alva‐Valdivia L M. ***Curie Temperatures and Emplacement Conditions of Pyroclastic Deposits from Popocatépetl Volcano, Mexico*** *[J] Geochemistry, Geophysics, Geosystems, e2022GC010340.*

https://doi.org/10.1029/2022GC010340

摘要：Popocatépetl 火山的大多数火山碎屑沉积是在高温下就位的，具有与高演化成分相似的镁铁质特征，表明存在长寿、相互关联的岩浆环境。我们对年龄<14 ky 的不同喷发序列进行了磁学和显微研究，发现温度和场依赖的磁化率可以区分喷发阶段。我们观察到居里温度（T_C）为 50-200 °C 和 200-400 °C 的均质钛磁铁矿，以及不同数量的 T_C 约 570 °C 的氧化出溶钛磁铁矿。一些块状和灰状沉积层展示出明显不可逆加热和冷却过程，其居里温度可以升高 130 ℃。该地层序列的中心部分的特征是磁化率降低和低的场依赖磁化率（<10%），这对于富含钛铁尖晶石的钛磁铁矿来说是不典型的。以约 10K/min 的速率测量可能与快速淬火过程中形成的空位增强的纳米级化学聚集或轻微的磁赤铁矿化相关的加热和冷却过程的不可逆性。相反，浮石层具有最高的场依赖性（~20%），其包含 T_C 分别为 100 与 300 ℃的高钛磁铁矿与中等钛含量的钛磁铁矿，这与镁铁质及更高演化的特征的岩浆相似。中间相 T_C 不可逆性更普遍，但其 T_C 小，约为±20 ℃。我们认为火山碎屑流内的磁性矿物是复杂的，但是给古地磁方向分析提供了关于其就位温度、就为条件及其火山物质的历史相关信息。

ABSTRACT: Most pyroclastic deposits of Popocatépetl volcano were emplaced at high temperatures, and have similar mafic to more evolved compositions, suggesting a long-lived, interconnected magma environment. We performed a magnetic and microscopic study on different eruptive sequences <14 ky in age and found that temperature- and field dependence of magnetic susceptibility is suited to separate eruption phases. We observed homogeneous titanomagnetite with Curie temperatures (T_C) of 50–200 °C and 200-400 °C, together with different amounts of oxy-exsolved titanomagnetite with T_C ~570 °C. Some block-and-ash flow deposits show remarkably

irreversible T_C in heating and cooling branches with a positive ΔT_C ($T_{C\ heating} - T_{C\ cooling}$) of up to 130 °C in the center. The central part of this sequence is characterized by decreasing magnetic susceptibility and low field dependence of magnetic susceptibility (<10%), which is atypical for ulvöspinel-rich titanomagnetite. The non-reversibility of heating and cooling runs measured with rates of around 10K/min is probably related to vacancy-enhanced nanoscale chemical clustering, which seems to occur preferentially during rapid quenching, possibly combined with subtle maghemitization. In contrast, pumice layers have the highest field dependence (~20%) and contain Ti-rich and intermediate titanomagnetite with T_C <100 and ~300 °C, which are in line with mafic and more evolved magma composition. In intermediate phases, irreversibility of T_C is more common but with a relatively low ΔT_C of ±20 °C. We suggest that magneto-mineralogy in pyroclastic density currents is complex but offers a complementary tool to paleomagnetic directional analysis for emplacement temperature and contribute information on the volcanic material history and their emplacement conditions.

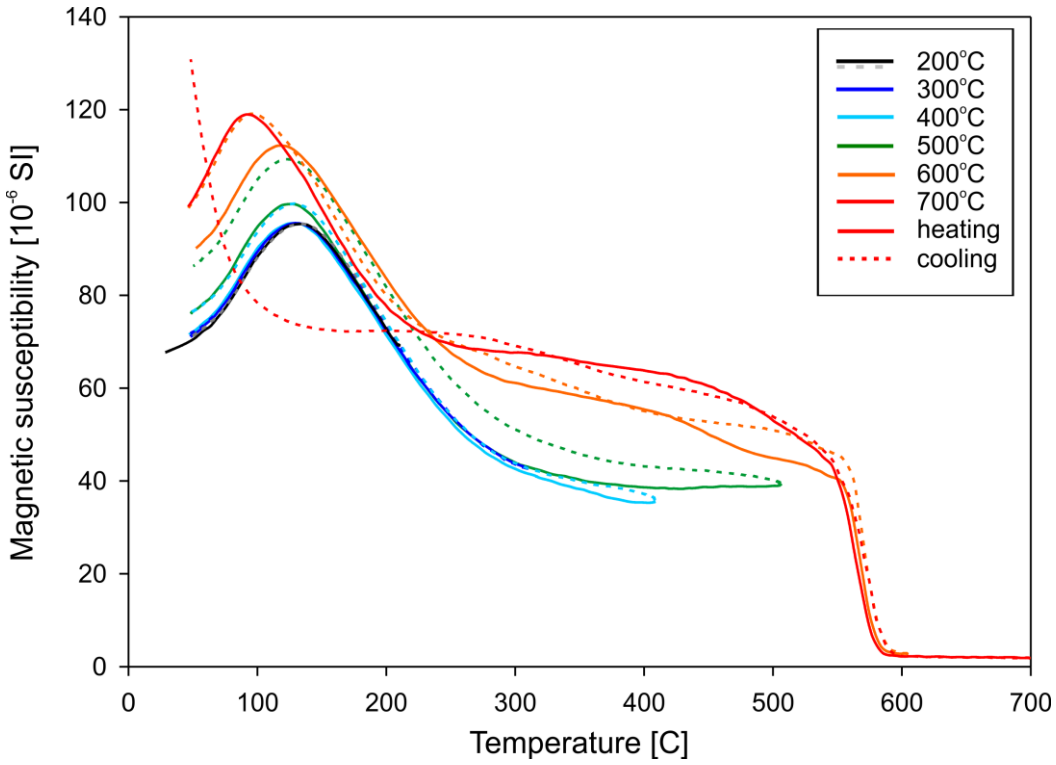

Figure 1. Repeated progressive heating-cooling cycles of sample POP4-80 at heating/cooling rates of 10 K/ min in 100°C steps up to 700°C (measured in argon). Solid and dashed lines indicate heating and cooling curves, respectively.

8. 自 11 Ma 以来撒哈拉沙漠的干旱受天文控制

翻译人：李海 12031330@mail.sustech.edu.cn

Crocker A J, Naafs B D A, Westerhold T, et al. ***Astronomically controlled aridity in the Sahara since at least 11 million years ago*** *[J] Nature Geoscience, 2022.*

https://doi.org/10.1038/s41561-022-00990-7

摘要：撒哈拉沙漠是地球上最大的热沙漠。然而，它开始的时间和其对气候强迫的反应存在争议，导致对区域干旱的原因和后果的不确定性。在本研究中，作者展示了从非洲到北大西洋沉积物的陆地输入的详细记录，记录了 1100 万年前湿润和干旱的撒哈拉沙漠之间的天文韵律振荡的长期且持续历史。研究结果表明，大陆中心的粉尘排放比北半球冰川作用的加剧和撒哈拉沙漠最古老的陆基证据早数百万年。北非没有向干旱的气候状态进行简单的长期渐进过渡，这表明干旱不是非洲大草原 C_4 草原逐渐扩大的新近纪扩张的主要驱动力。相反，在过去的 11 Ma 中，太阳辐射驱动的撒哈拉气候干湿变化很常见，并确定了这种关系敏感性的三个不同阶段。本文的数据为非洲的生物演化结果提供了背景；例如，研究结果表明天文学上步调一致的干旱间隔比古人类两足动物最古老的化石证据至少早 4 Ma。

ABSTRACT: The Sahara is the largest hot desert on Earth. Yet the timing of its inception and its response to climatic forcing is debated, leading to uncertainty over the causes and consequences of regional aridity. Here we present detailed records of terrestrial inputs from Africa to North Atlantic deep-sea sediments, documenting a long and sustained history of astronomically paced oscillations between a humid and arid Sahara from over 11 million years ago. We show that intervals of strong dust emissions from the heart of the continent predate both the intensification of Northern Hemisphere glaciation and the oldest land-based evidence for a Saharan desert by millions of years. We find no simple long-term gradational transition towards an increasingly arid climate state in northern Africa, suggesting that aridity was not the primary driver of gradual Neogene expansion of African savannah C_4 grasslands. Instead, insolation-driven wet–dry shifts in Saharan climate were common over the past 11 Myr, and we identify three distinct stages in the sensitivity of this relationship. Our data provide context for evolutionary outcomes on Africa; for example, we find that astronomically paced arid intervals predate the oldest fossil evidence of hominid bipedalism by at least 4 Myr.

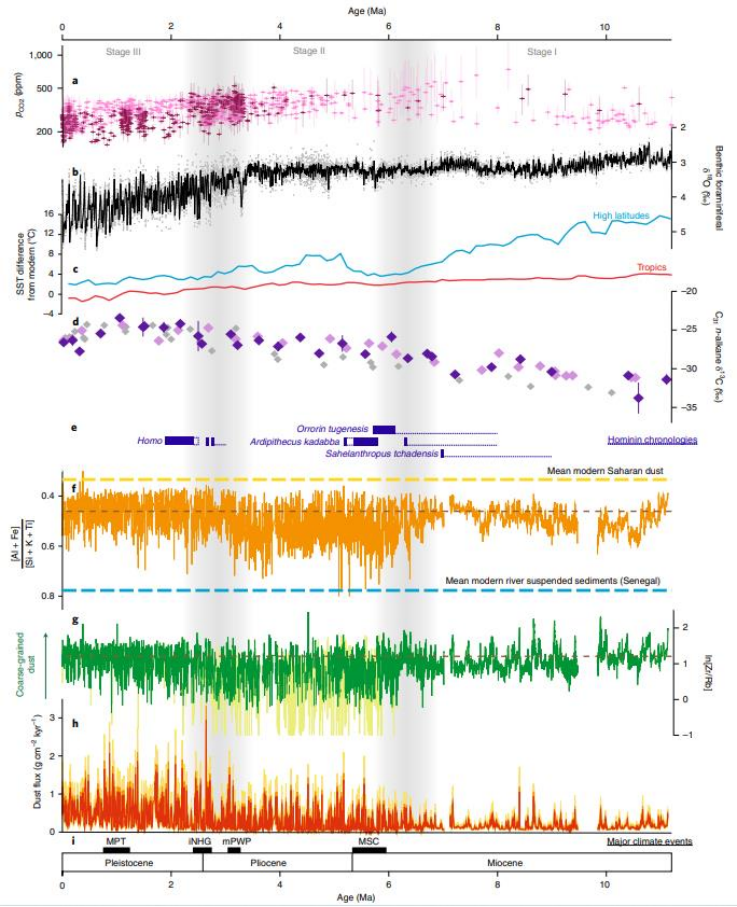

Figure 1. African hydroclimate compared with global change over the past 11 Myr. a, Atmospheric pCO_2 reconstructions (references in Supplementary Information): purple, estimates from planktonic foraminiferal boron isotopic signatures; pink, alkenone-derived estimates. b, Cenozoic global reference benthic foraminifera oxygen isotope dataset, with 20 kyr smoothing[29]. c, Regional stacks of sea surface temperature (SST) difference from modern annual means[23]: blue, >50° N; red, tropics. d, $\delta^{13}C$ signature of n-alkanes from Site 659 (dark purple, this study; light purple, ref. 36) and offshore East Africa[48] (grey). Error bars indicate 1σ. e, Major events in hominid evolution. Solid bars are taxon ranges; dashed lines represent confidence interval on taxon origin[47]. f, [Al + Fe]/[Si+K + Ti] of calibrated elemental abundances. Modern endmember values updated from ref. 17 (Supplementary Information). Brown dashed line marks mean over past 1 Myr. g, ln[Zr/Rb] XRF core scan ratios. Dashed line marks mean over past 1 Myr. h, Site 659 estimated dust flux (3-point smoothed). Median value in red; 1st, 5th, 25th, 75th, 95th and 99th percentiles also shown in shades of orange/yellow. i, Major global climate events. MPT, mid-Pleistocene transition; iNHG, intensification of Northern Hemisphere glaciation; mPWP, mid-Pliocene warm period; MSC, Messinian salinity crisis. Vertical grey shading indicates transitions between climate stages.

9. 西南极洲太平洋边缘的边界过程和钕循环

翻译人：张亚南 zhangyn3@mail.sustech.edu.cn

Wang R, Willianms T, Hillenbrand C-D, et al. ***Boundary processes and neodymium cycling along the Pacific margin of West Antarctica*** *[J] Geochimica et Cosnochimica Acta, 2022, 327, 1-20. https://doi.org/10.1016/j.gca.2022.04.012*

摘要：钕（Nd）同位素在现代海洋和古海洋学研究中被用作水团来源的示踪剂。尽管海洋 Nd 循环还没有被完全限制。最近研究强调了发生在海洋-沉积物界面的过程对于改变底层水 Nd 同位素组成具有重要作用。边界交换和交换通量是影响水团性质的 2 个主要过程，但还需要对其化学机制及影响程度进行更多的研究。由于南极源水主导着南大洋，并调控全球大洋深水通风，因此南极大陆边缘成为研究这些过程的重要场所。这次研究首次测量和对比了南极洲大陆边缘海水、孔隙水和沉积物数据，来研究潜在边界过程的性质。作者认为，在孔隙水中似乎发生了类似于边界交换的过程，改变孔隙水 Nd 同位素比值（更具放射性），而不显著增加溶解 Nd 浓度。作者推测，这种改变是由于放射性碎屑颗粒的部分溶解（如：蒙脱石、角闪石或火山玻璃），而后在通过再清除维持低 Nd 浓度。作者通过研究孔隙水中的化学梯度推断出孔隙水到深水间的交换通量，与其他研究相比，南极边缘的交换通量要低得多。由于有机颗粒的部分降解和与之相关的 Fe-Mn 氢氧化物的溶解，沿南极半岛的交换通量要略高于 Bellingshausen 海。综上所述，边界过程并未显著改变南极边缘海的 Nd 同位素组成，这是因为，尽管孔隙水的 Nd 组成发生了改变，但与其他环境相比，其 Nd 浓度较低。

ABSTRACT: Neodymium (Nd) isotopes have been utilized as a tracer of water mass source in the modern ocean and in palaeoceanographic studies, though the oceanic cycling of Nd is not yet fully constrained. Recent studies have highlighted the importance of processes that occur near the seawater – sediment interface in altering the Nd isotopic composition of bottom waters. The two major observed processes “boundary exchange” and “benthic flux” have been suggested as playing an important role in setting water mass compositions, however, more studies are needed to constrain their chemical mechanism and the extent to which these processes set the composition of deep waters. The Antarctic continental margin is an important place to study these processes because

Antarctic-sourced waters dominate the Southern Ocean and ventilate the global deep ocean. This study is the first to measure and compare seawater, porewater and sediment data from along the margin of Antarctica to examine the nature of potential boundary processes. We show that a process similar to boundary exchange seems to be occurring within porewaters, modifying porewater chemistry by shifting its Nd isotopic ratios to more radiogenic values without significantly increasing the concentration of dissolved Nd. We hypothesize that this shift results from partial dissolution of radiogenic detrital particles, such as smectite, amphibole and/or volcanic glass, while re-scavenging maintains low Nd concentrations. We infer the existence of benthic flux of porewaters to deep waters by examining chemical gradients in porewaters and show that it is much lower on the Antarctic margin compared to other studies. Benthic flux appears to be slightly higher along the Antarctic Peninsula than in the Bellingshausen Sea due to partial degradation of organic matter and associated dissolution of Fe-Mn oxyhydroxides. Taken together, boundary processes do not significantly change the Nd isotopic composition of Antarctic margin seawater because while the porewaters have an altered Nd isotopic composition the Nd concentration of these porewaters is low compared to other settings.

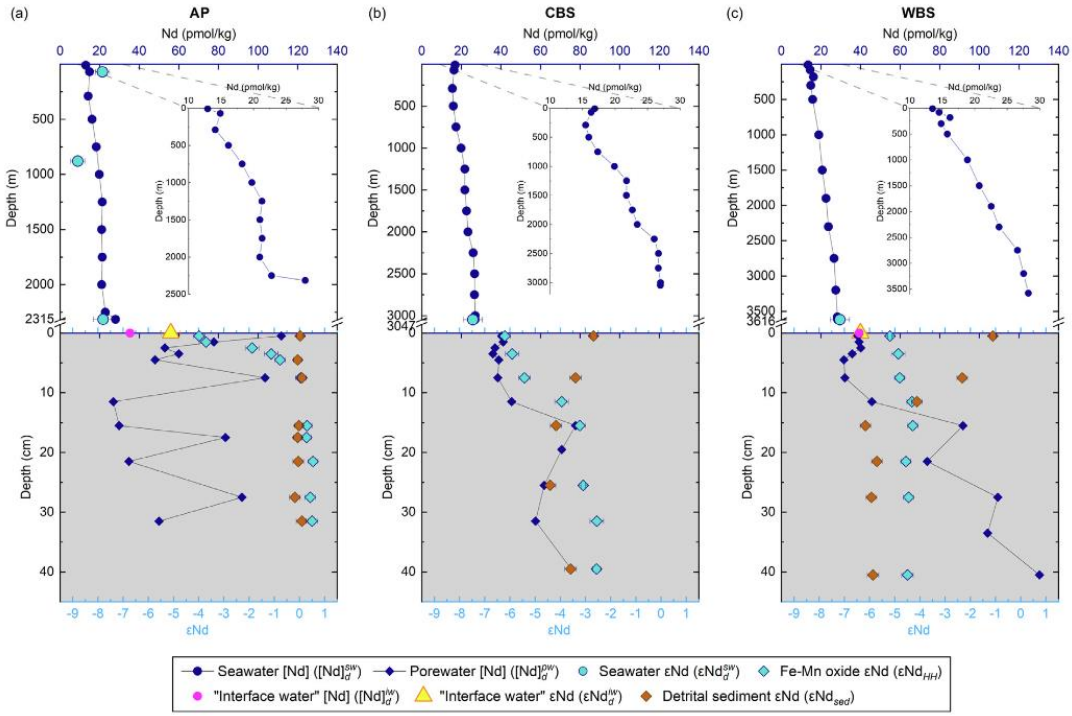

Figure 1. Nd concentrations and Nd compositions of combined seawater, porewater and fine-grained detrital sediments at the studied sites (a) AP, (b) CBS, and (c) WBS. The εNd composition

of porewater could not be measured directly but is inferred from the εNd composition of authigenic Fe-Mn coatings. The inset figure at each site shows the seawater Nd concentration profiles on an enlarged scale.

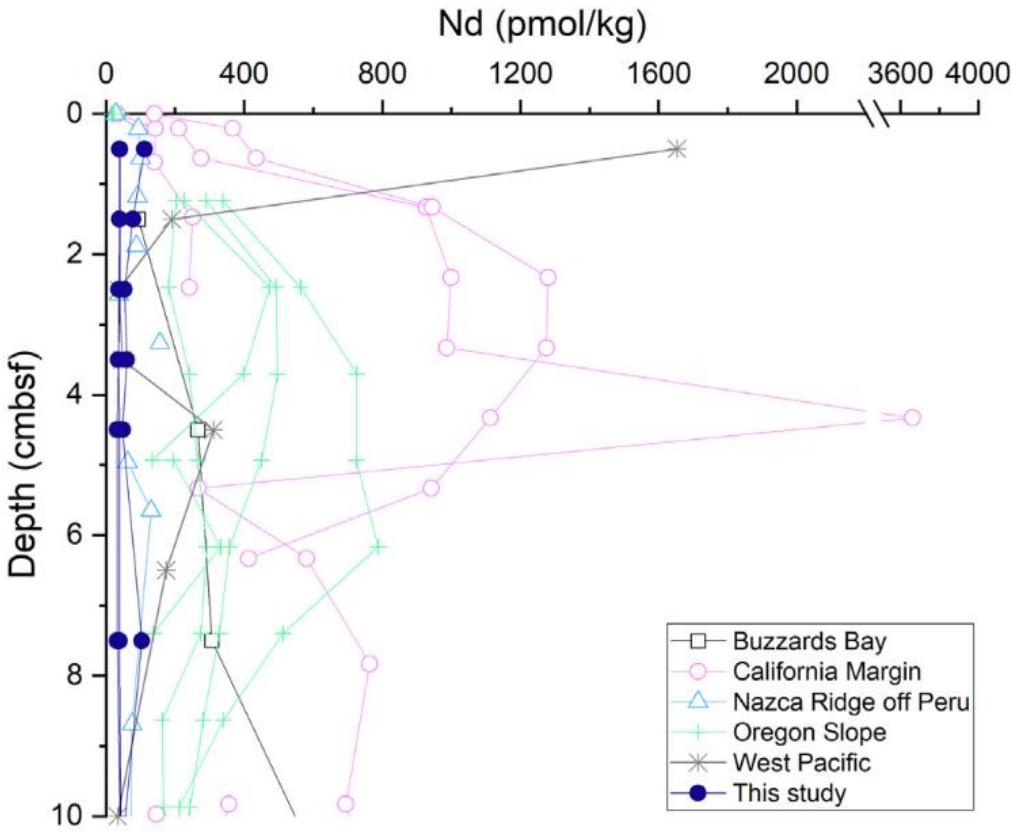

Figure 2. Global data comparison of dissolved Nd concentrations in porewater within the upper 10 cm of the seabed. Data source: Buzzards Bay, east coast of North America, from Sholkovitz et al. (1989); California margin and Nazca Ridge off Peru from Haley et al. (2004); Oregon slope from Abbott et al. (2015a); West Pacific from Abbott (2019).

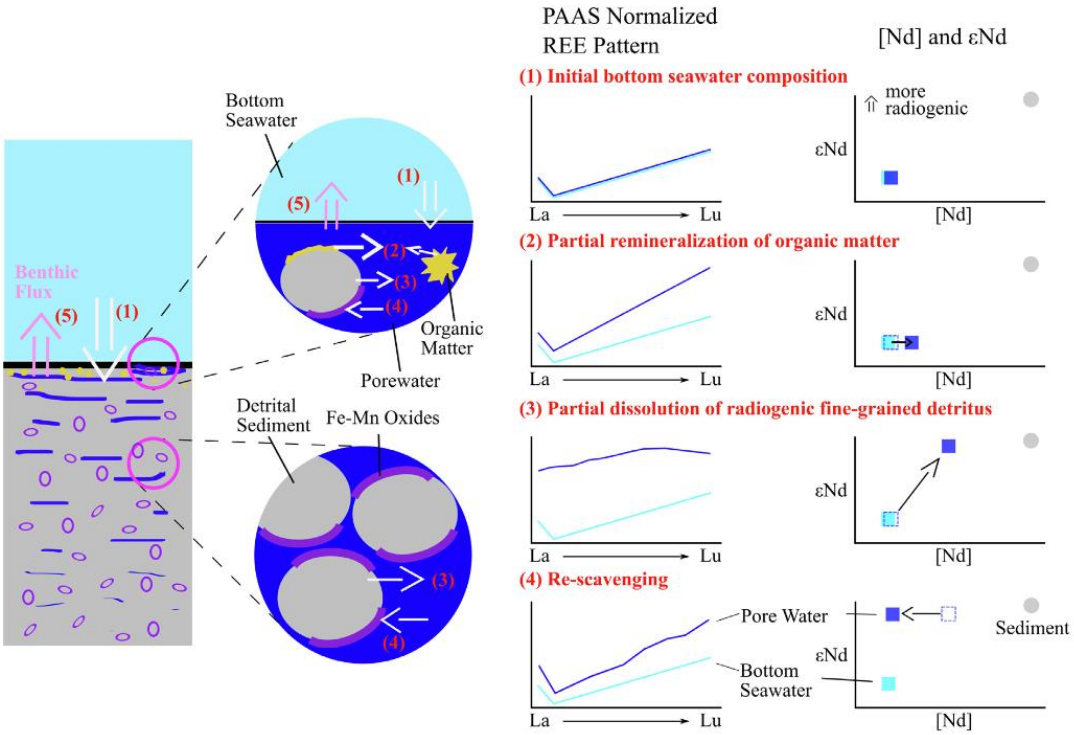

Figure 2. Schematic description of boundary processes on the West Antarctic continental margin. The four steps of boundary processes are illustrated in the cartoons on the left; and the corresponding changes of REE patterns, [Nd] and εNd with every step are shown in the right panels.

10. 在大洋中脊回收太古宙克拉通地幔

翻译人：刘宇星 11811211@mail.sustech.edu.cn

Liu C Z, Dick H J B, Mitchell R N, et al. ***Archean cratonic mantle recycled at a mid-ocean ridge*** *[J] Science Advances, 2022, 8(22), eabn6749.*

https://doi.org/10.1126/sciadv.abn6749

摘要：大洋中脊的玄武岩和地幔橄榄岩被认为是代表地球上地幔的样本。深海橄榄岩的锇同位素独特地保存了整个地球历史上的熔体提取事件，但现有记录仅表明大约 20 亿年前(2 Ga)前的年龄。因此，在太古代(>2.5 Ga)存在的疑似大量地幔岩石圈的记录不明原因地丢失了。我们发现了熔体耗尽年龄高达 2.8 Ga 的深海橄榄岩，有极非放射性的 $^{187}Os/^{188}Os$ 比率（低至 0.1095）和组成类似于太古代克拉通的难熔主要元素记录。因此，这些海洋岩石来自曾经广阔的太古代大陆克拉通，这些克拉通残片已经被移出并循环回地幔，我们通过数值模型证实了其可行性。年轻的海洋和古老的大陆岩石圈之间的这种意想不到的联系表明，随着时间的推移，地壳成分循环的程度被低估了。

ABSTRACT: Basalts and mantle peridotites of mid-ocean ridges are thought to sample Earth's upper mantle. Osmium isotopes of abyssal peridotites uniquely preserve melt extraction events throughout Earth history, but existing records only indicate ages up to ~2 billion years (Ga) ago. Thus, the memory of the suspected large volumes of mantle lithosphere that existed in Archean time (>2.5 Ga) has apparently been lost somehow. We report abyssal peridotites with melt-depletion ages up to 2.8 Ga, documented by extremely unradiogenic $^{187}Os/^{188}Os$ ratios (to as low as 0.1095) and refractory major elements that compositionally resemble the deep keels of Archean cratons. These oceanic rocks were thus derived from the once-extensive Archean continental keels that have been dislodged and recycled back into the mantle, the feasibility of which we confirm with numerical modeling. This unexpected connection between young oceanic and ancient continental lithosphere indicates an underappreciated degree of compositional recycling over time.

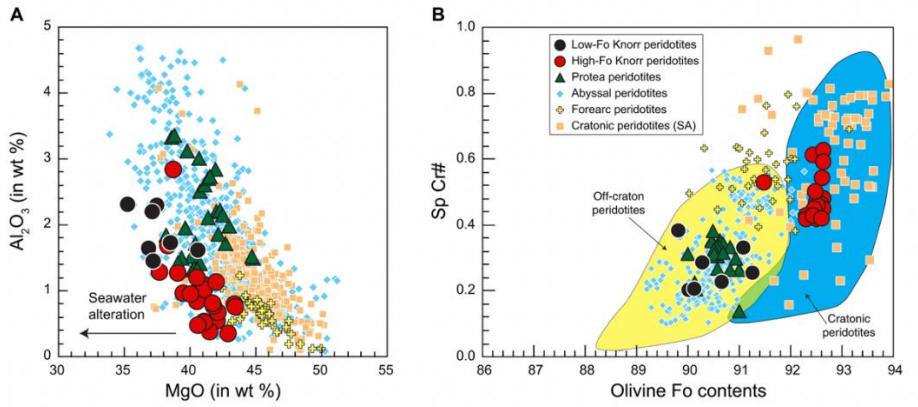

Figure 1. Geochemistry of SWIR abyssal peridotites. (A) Whole-rock MgO versus Al_2O_3. (B) Olivine Fo contents versus spinel Cr# values. Fields of cratonic and off-craton peridotites are from (56). Data sources of abyssal peridotites, forearc peridotites, and South African (SA) cratonic peridotites are from the PetDB database (www.earthchem.org/petdb).

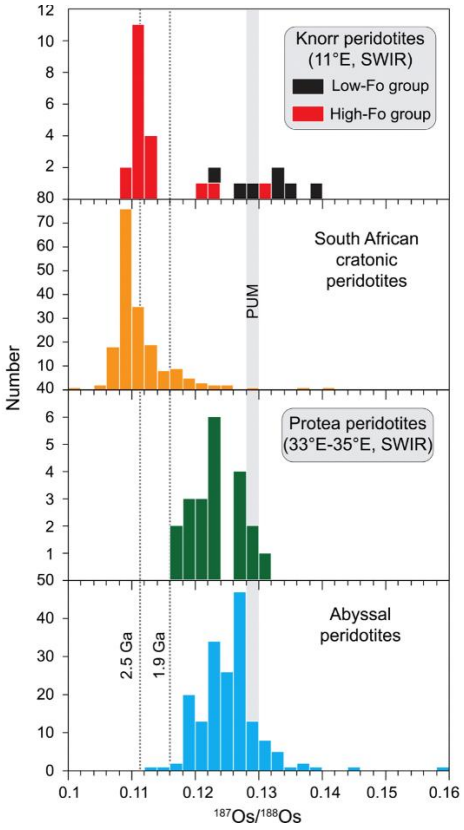

Figure 2. Whole-rock $^{187}Os/^{188}Os$ ratios of SWIR abyssal peridotites. Two dashed lines refer to T_{RD} ages of 2.5 and 1.8 Ga, which were calculated relative to the PUM (20). Data of abyssal peridotites are from (2–5, 8, 21), and data of mantle xenoliths from Kaapvaal and Zimbabwe cratons are from (19, 57–64). The higher $^{187}Os/^{188}Os$ ratios of SWIR peridotites than those of the PUM might be due to interaction with seawater (21).